Systems & Control Transactions

Research Article
Foundations of Computer Aided Process Design (FOCAPD 2024)
Breckenridge, Colorado, USA. July 14-18, 2024
Peer Reviewed Conference Proceeding

PSE PRESS

Optimal Design and Control of Behind-the-Meter Resources for Retail Buildings with EV Fast Charging

Gustavo Campos[a,*], Roberto Vercellino[a], Darice Guittet[a], Margaret Mann[a]

[a] National Renewable Energy Laboratory (NREL), Golden, CO, USA
* Corresponding Author: gustavo.campos@nrel.gov

ABSTRACT

The growing electrification of buildings and vehicles, while a natural step towards achieving global decarbonization, poses some challenges for the electric grid in terms of power consumption. One way of addressing them is by deploying onsite, behind-the-meter resources (BTMR), such as battery energy storage and solar PV generation. The optimal design of these systems, however, is a demanding task that depends on the integration of multiple complex subsystems. In this work, the optimal integrated design and dispatch of BTMR systems for retail buildings with electric vehicle fast charging stations is addressed. A framework is proposed, combining high-fidelity simulation (of buildings, electric vehicle fast charging stations, and BTMR), predictive control strategies with closed-loop implementation, and a derivative-free design method that explores parallelization and high-performance computing. Focus is given to the design layer, highlighting the effect of parallelization on the choice of the method, computational effort, and types of results. A case study of a big-box grocery store with an EV fast charging station is presented, and its optimal BTMR system is identified in terms of equipment sizes, costs (capital, utility, lifecycle, and levelized) and resiliency against outages, demonstrating great potential for real-world applications.

Keywords: Battery Energy Storage, Distributed Generation, Electric Vehicle Fast Charging, Model Predictive Control, Derivative-free Optimization.

INTRODUCTION

Electrification is held as one of the fundamental pillars for achieving widespread decarbonization, especially for historically fuel-dominated sectors such as transportation (now the largest contributor to greenhouse gas emissions in the United States [1]). This trend, however, comes with its own challenges. Widespread electrification will generate loads not seen in the past – a single electric vehicle (EV) fast charger can have a comparable load to an entire commercial building or hundreds of single-home residences, while a fast charging station can overshadow its building counterpart [2]. These loads, if not addressed adequately, will incur hefty penalties in the form of utility charges and power distribution upgrades.

One way of reducing the peak demand and overall energy consumption of these systems is by employing onsite, distributed, behind-the-meter (BTM) resources (BTMR), such as energy storage and generation – battery storage and solar PV generation being the most notable examples – as shown in Figure 1. This allows the system to generate renewable solar energy during the day and store it for later when either demand or prices are high (reducing both energy and demand charges), as well as to reduce the peak demand by charging the battery in advance and using it instead of the grid to meet the system's demand (reducing demand charges).

The design of BTMR systems, however, is a challenging task integrating multiple time scales, complex subsystems and application-specific parameters (e.g., expected building and EV charging loads, climate data, utility tariff, and power distribution capacity). The most cost-effective design of such systems also depends on their day-to-day operation in response to all these factors over long time periods. Moreover, the high variability of loads such as for EV fast charging requires a high-resolution time step to accurately predict system sizes.

Several tools and works have addressed this problem in the past. REopt [4], DER-CAM [5], and DER-VET [6] are examples of free software tools, while HOMER and

Energy Toolbase are examples of commercial software. The majority of these tools employ a structured, mixed-integer linear programming (MILP) optimization framework that solves an integrated design and dispatch problem. This allows the representation of a large variety of technologies [4], buildings and microgrid configurations [5, 6], but hinder accuracy. The building (and EV charging) loads are typically treated as exogeneous inputs, obtained from historical records or pre-computed hypothetical profiles. Detailed simulation models, essential for capturing equipment performance and financial mechanisms and validating the solutions generated by the simplified dispatching models, are not supported. The closed-loop implementation of the control solutions is also a critical missing component, overlooking forecast errors and their associated limitations (the projection of peak demand charges over the following month being one of the biggest challenges). Lastly, 1 minute time discretization, required to capture EV fast charging dynamics, are difficult to implement (using a year-long horizon, necessary for solar generation) without facing scalability issues.

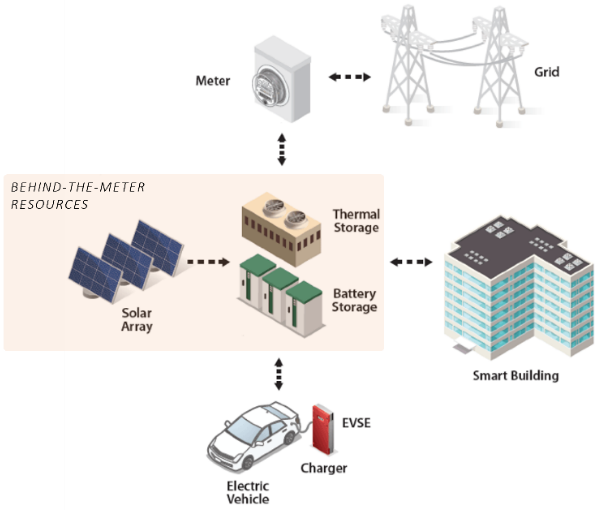

Figure 1. Diagram of behind-the-meter resources. (adapted from [3])

To address these limitations, a novel framework is proposed for simulation-based design of BTMR. This framework is used as the basis for the NREL tool EVI-EDGES (Electric Vehicle Infrastructure - Enabling Distributed Generation and Energy Storage) [7].

METHODOLOGY

An overview of the methodology framework is presented in Figure 2. Each individual component is described in the following subsections.

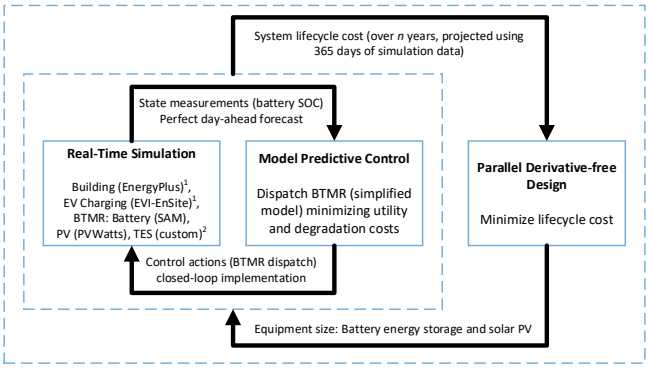

[1] *Electrical loads can be pre-computed depending on the level of detail required*
[2] *Not included in this work*

Figure 2. Methodology for sizing behind-the-meter resources.

Simulation

The simulation environment is composed by three main components: building, electric vehicle charging station, and BTMR (battery energy storage, PV, thermal storage). In its simplest form, the first two models can be pre-solved before running the framework (for instance, when solving the base case without BTMR), while the third group of models needs to be solved in real-time with the control layer. When thermal storage (either active or passive) is present (in other words, when the operation of building cooling and heating equipment can be shifted in time), the building load depends on the BTMR dispatch and can no longer be detached and pre-simulated [8]. Thus, ideally, all the models would be integrated and solved simultaneously, allowing the consideration of interaction effects between them (e.g., battery thermal gain affecting the building indoor temperature, or EV charging schedule affected by the buildings loads).

Building

The building thermal and electrical loads are generated using EnergyPlus (U.S. Department of Energy, 2023), a whole building energy simulation program with a rich database of construction material properties that allows the accurate representation of interactions between building zones and environment, and its resulting energy consumption (e.g., heating, cooling, ventilation, lighting, and plug loads). In its most general form, the framework allows passing operating setpoints from the control block to the building simulation, scheduling the operation of electrically-driven HVAC equipment such as chiller or heat pumps, in turn affecting the building's electrical load. The battery is placed inside of one of the building's zones with temperature control, modeling thermal interaction that determines zone cooling loads as well as battery thermal degradation and effects.

Electric Vehicle Charging Station

The EV fast charging station is simulated using an

agent-based model (NREL's EVI-EnSite [9]). Input data includes probability distributions of vehicle arrival time and arrival state-of-charge (SOC), the number of vehicle arrivals per day or week, as well as general vehicle type-related characteristics, such as battery size and charge acceptance curves (power x SOC). The vehicle charging process is simulated by assigning arriving vehicles to unoccupied charging ports following a certain metric (usually either first-in-first-out, or a managed-charging schedule based on cost minimization). In case all charging ports are occupied, the arriving vehicles are queued and must wait in order to charge. Typically, the charging station design (i.e., number of charging ports and charging port power level) is performed to minimize the queueing time distribution (mean or a certain percentile), the latter constructed empirically by repeatedly sampling the input distributions in a Monte-Carlo fashion.

BTMR: Battery Energy Storage and PV

A detailed technoeconomic BTM battery storage model from NREL's System Advisor Model (SAM) [10] is employed to simulate the real system's performance (as opposed to the simplified battery model inside of the MPC formulation). This model is able to represent different battery types (lithium-ion, lead-acid, redox flow) and multiple chemistries of lithium-ion batteries (LMO, LTO, LCO, LFP, NMC, NCA) with associated typical voltage curves, thermal behavior, and lifetime degradation profiles.

The solar PV panels are modeled using NREL's PVWatts model [11, 12], which considers a grid-connected photovoltaic system with modules/panels composed by crystalline silicon or thin film photovoltaic cells. Inputs related to the system's physical characteristics include power capacity, module and array types, losses, array orientation (angles) and mounting type, as well as a few built-in module and inverter characteristics.

Optimal Dispatch/Control

The battery dispatch/control problem is formulated as a Linear Programming (LP) model (Nonlinear Programming depending on the type of battery degradation considered [13], or Mixed-Integer Nonlinear Programming if thermal storage is included [8]). This problem optimizes the adjusted cost of operation of the system (utility costs and battery degradation). A condensed formulation of the LP problem is presented next:

$$\min \phi = C^E + C^D + C^R \quad (1)$$

subject to

$$C^E = \Delta t \sum_t \phi_t^E (P_t^{purch} - \gamma^{nm} P_t^{sold}) \quad (2)$$

$$C^D = \sum_d \phi_d^D \bar{P}_d^{max} \quad (3)$$

$$C^R = \left(E^{max} - E_{t=t_f}^h\right)(RCP * EPR + RCE) \quad (4)$$

$$-P_t^{load} + P_t^{pv} + \left(P_t^{purch} - P_t^{sold}\right) + \left(P_t^{out} - P_t^{in}\right) = 0 \quad (5)$$

$$E_t - E_{t-1} = \Delta t\left(\eta^{in} P_t^{in} - \eta^{out} P_t^{out}\right) \quad (6)$$

$$E_{t=t_0}^h S^{min} \le E_t \le E_{t=t_0}^h S^{max} \quad (7)$$

$$E_{t=t_f}^h = E^{max} - DE_{t=t_f}^{tp} \quad (8)$$

$$E_{t=t_f}^{tp} = E_{t=t_i}^{tp} + \frac{\Delta t}{2}\sum_t \left(P_t^{in} + P_t^{out}\right) \quad (9)$$

$$\bar{P}_{\bar{t}}^{purch} = \frac{\Delta t}{\Delta \bar{t}} \sum_{t \in T_{\bar{t}}} P_t^{purch} \quad (10)$$

$$\bar{P}_d^{max} \ge \bar{P}_{\bar{t} \in \bar{T}_d}^{purch}, \ \bar{P}_d^{max} \ge \bar{P}_d^{max,i} \quad (11)$$

where **indices** include the time step $t \in T$ (initial and final time steps t_i and t_f); 15-min average time step $\bar{t} \in \bar{T}$; and demand charge periods $d \in D$. **Special sets** include $T_{\bar{t}}$ (all time steps t inside of each 15-min average time step $\bar{t}$); and $\bar{T}_d$ (all average time steps $\bar{t}$ inside of each demand period d).

Parameters include the difference between time steps Δt and $\Delta \bar{t}$ (hours); battery installed cost per power ICP ($/kW) and per energy ICE ($/kWh); battery replacement cost per power RCP ($/kW) and per energy RCE ($/kWh); time-of-use energy prices ϕ_t^E and demand prices ϕ_d^D; net-metering factor (representing the lesser value of selling power to the grid as opposed to purchasing it) γ^{nm} (decimal); battery charging and discharging efficiencies η^{in} and η^{out} (decimal), battery degradation per energy throughput D (decimal/kWh); energy to power ratio EPR (kWh/kW) (from design layer); minimum and maximum state-of-charge S^{min} and S^{max} (decimal); and the 15-min peak power demand from the previous day for each demand charge period $\bar{P}_d^{max,i}$ (kW). **Forecasted parameters** include the system electrical load (sum of building and EV charging) P_t^{load} (kW), and PV generation P_t^{pv}(kW).

Variables include the battery power charged and discharged P_t^{in} and P_t^{out} (kW); the battery energy E_t (kWh), throughput E_t^{tp} (kWh), and health E_t^h (decimal); power purchased from and sold to the grid, P_t^{purch} and P_t^{sold} (kW); 15-min average purchased power $\bar{P}_t^{purch}$ and maximum purchased power in each demand period $\bar{P}_d^{max}$ (for demand charge calculations). All variables are non-negative reals.

The **objective function** (1) minimizes energy cost C^E ($), demand cost C^D ($), and battery replacement cost C^R ($). **Constraints** include cost calculations (2-4); power balance (5); battery energy storage difference equation (6); battery energy bounds based on its health (7); battery health at the end of the control window as a function of its energy throughput (8); battery energy throughput definition (9); 15-min averaging of power purchased from the grid (10); and 15-min peak demand power calculation (11).

A control horizon of 1 day is used (typical for short-duration energy storage problems with diurnal patterns), with a recalculation frequency of 1 day and a time step discretization of 1 minute to accurately capture the high variability from EV charging loads (battery and power distribution must be sized with the instantaneous load instead of averages). After each horizon is solved, a time series of control setpoints is provided to the simulation for evaluating the response of the subsystems and updating the stationary battery health. Then the final system state from the simulation is set as initial point of the successive control problem.

Optimal Design

Under the formulation described above, the overall design problem can be posed as a nested optimization problem, in which each evaluation of the design layer depends on the solution of a lower-level layer consisting of several coupled control optimization subproblems, further complicated by their closed-loop implementation in the simulation environment. The objective function (system lifecycle cost) is also time-consuming to evaluate (in the order of hours), which makes approximating the derivatives via finite-difference methods an ineffective approach. For these reasons, only derivative-free (black-box) optimization methods were considered [14, 15].

These methods are generally classified according to the properties of the black-box oracle function [15], which in the present case is assumed to be deterministic, generally nonconvex and non-smooth, multimodal (although empirically observed to be unimodal), unconstrained, with bounded feasible region (decision variables are typically nonnegative real variables, with upper bounds determined from space and weight constraints or heuristics), and time-consuming evaluation (hours). The latter is a key characteristic that prohibits or hinders the application of direct-search methods such as Nelder-Mead (with a low number of simplex vertices) or trust-region methods, which require several iterations to converge.

The ability to parallelize (concurrent) function evaluations is considered as a critical feature to determine the choice of method. Most optimization methods tend to minimize the total number of function evaluations over the entire algorithm, as opposed to minimizing the time required to solve the problem (typically proportional to each other). When each function evaluation is time consuming, however, it is more efficient to parallelize as many concurrent evaluations as possible, then use the ensemble information to perform the search.

Sequential Grid Search Method

A sequential grid search method is employed, which samples the decision space using symmetric hypercubes that begin by covering the whole feasible space and shrink around the observed optimum after each iteration. In other words, after each iteration, the optimum point is identified between two (if the solution lies at the bounds) or three (if it falls in the middle) grid points in each direction, which are set as the new bounds for the reduced grid at the next iteration (previously evaluated points are reused for the new grid to reduce effort). The number of function evaluations for each iteration depends on the number of discrete points in each of the grid's independent coordinates (variables). For a problem with three decision variables, the number of evaluations will then be equal to the number of points to the power of three. This points out the major deficiency of this approach, which is its scalability with the number of decision variables. While it is efficient for this problem setup, it becomes more challenging when including other design variables (e.g., TES or charging station). The method is illustrated in Figure 3, showing the evolution of the grid and optimal point throughout subsequent iterations.

After each iteration, a surrogate model can be fitted and the next-iteration grid can be generated around the surrogate optimum instead of the sampled one. However, the benefit of this approach is not guaranteed, as it depends on how well the surrogate represents the real underlying function. If the surrogate model does not capture the function appropriately, it can mislead the search and affect it negatively, adding iterations and increasing the runtime. It was empirically observed that low order polynomial models do not add a significant value in predicting the true optimum location and were thus not employed.

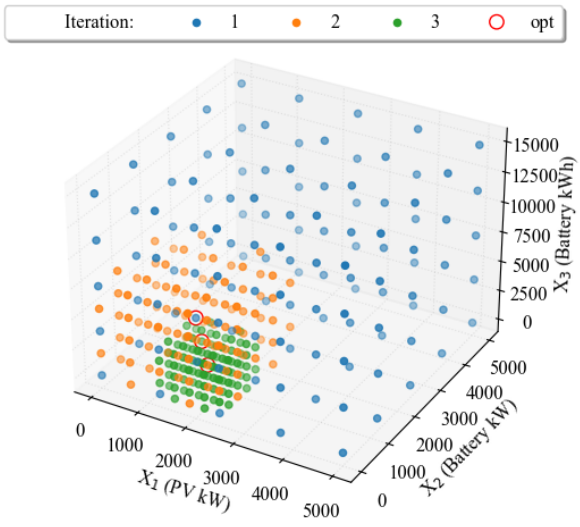

Figure 3. Illustration of a 3-dimensional sequential grid search with 5 points in each direction and 3 iterations. used to interpolate the optimum location.

Accuracy and Computational Effort

The upper bound on the final accuracy level δx_{n_i} (difference between two evaluated points) after n_i

iterations, using n_p points in each direction (assuming the same number of points for all directions), and starting with an initial range Δx_0, is given in (12). Solutions obtained at the grid boundaries at any iteration will have a better accuracy due to its one-sided shrinkage (as opposed to two-sided shrinkage necessary for non-boundary solutions).

$$\delta x_{n_i} = \frac{(2^{n_i-1}\Delta x_0)}{(n_p-1)^{n_i}} \quad (12)$$

Two ways of refining the solution accuracy consist in increasing the number of evaluation points (n_p) or number of iterations (n_i). To guide the parameter tuning decision, the final solution accuracy (relative to the initial range Δx_0) and computational effort (in terms of core-hours, a typical measure for HPC systems) are presented in Table 1. It is assumed that each design evaluation point (one year simulation with closed-loop optimal control) has a runtime of approximately 2 hours, and that the number of cores equals the number of evaluated design points. Cells with final solution accuracy under 1% of the initial range are highlighted in bold in both tables.

Table 1: Solution accuracy and computational effort over varying number of grid points (cols) and iterations (rows).

n_p	4	5	6	7	8	9	10	
n_i	Final Solution Accuracy (Upper Bound on Error Margin)							h
1	33.3%	25.0%	20.0%	16.7%	14.3%	12.5%	11.1%	2
2	22.2%	12.5%	8.0%	5.6%	4.1%	3.1%	2.5%	4
3	14.8%	6.3%	3.2%	1.9%	1.2%	**0.8%**	**0.5%**	6
4	9.9%	3.1%	1.3%	**0.6%**	**0.3%**	0.2%	0.1%	8
5	6.6%	1.6%	**0.5%**	0.2%	0.1%	0.0%	0.0%	10
6	4.4%	**0.8%**	0.2%	0.1%	0.0%	0.0%	0.0%	12
7	2.9%	0.4%	0.1%	0.0%	0.0%	0.0%	0.0%	14
8	2.0%	0.2%	0.0%	0.0%	0.0%	0.0%	0.0%	16
9	1.3%	0.1%	0.0%	0.0%	0.0%	0.0%	0.0%	18
10	**0.9%**	0.0%	0.0%	0.0%	0.0%	0.0%	0.0%	20
	Computational Effort (Core-Hours)							
1	128	250	432	686	1024	1458	2000	2
2	256	500	864	1372	2048	2916	4000	4
3	384	750	1296	2058	3072	**4374**	**6000**	6
4	512	1000	1728	**2744**	**4096**	5832	8000	8
5	640	1250	**2160**	3430	5120	7290	10000	10
6	768	**1500**	2592	4116	6144	8748	12000	12
7	896	1750	3024	4802	7168	10206	14000	14
8	1024	2000	3456	5488	8192	11664	16000	16
9	1152	2250	3888	6174	9216	13122	18000	18
10	**1280**	2500	4320	6860	10240	14580	20000	20

For the presented setup, the number of grid points should be equal or greater to 5 (using 4 points requires at least 10 iterations, which would entail 20 hours of runtime), while the appropriate number of iterations varies between 3 and 6 (runtime of 6 and 12 hours). The bottom table shows that computational effort increases more rapidly with the number of grid points (total number of evaluations/cores per iteration is given by n_p^3) than iterations, although the latter increases runtime linearly by 2 hours. The final setup (grid coarseness and number of iterations) should thus be a function of several factors, including required solution time, number of parallel cores available, and acceptable solution accuracy.

In summary, a few conditions that encourage the application of this method include time-consuming objective function evaluation (in the order of hours); small number of design variables (up to 3 or 4); high parallelization (100s of concurrent function evaluations); bounded feasible region; and an acceptable final solution accuracy within 1% of initial range.

CASE STUDY

Building Model

A big-box grocery store building energy model, developed and validated in [2], was employed in this work. This represents a common type of commercial building in the United States, at which EV fast charging stations are expected to be increasingly deployed in the near future – fast charging stations in retail buildings will attract customers and bring additional revenue, increasing business competitiveness, while also providing charging access to disadvantaged areas with lacking access to home charging. The building model has 18 thermal zones, 136 surfaces, and 263 sub-surfaces (e.g., windows, doors), and an area of approximately 20,000 m^2. Figure 4 presents the 3D model of the building, with different zones roughly separated by solid roof lines, while the electrical load generated by the building (from HVAC and plug loads) is presented in Figure 5.

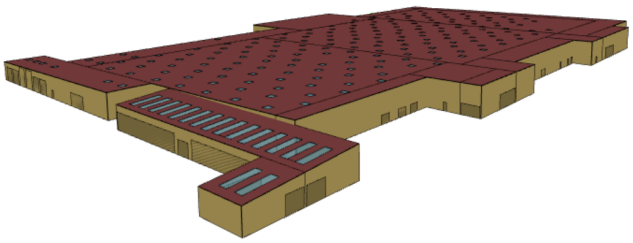

Figure 4. 3D model of the generic big-box grocery store from OpenStudio.

Electric Vehicle Charging Loads

A fast charging station with two 150 kW charging ports and 6 events per port per day was simulated. The load profile is presented in Figure 6. Default inputs for commonly used EVs were employed (vehicle battery size, charge acceptance curves), while the probability distributions (vehicle arrival time and SOC) were correlated to the building occupation patterns. The load has a high variability (spikiness), which may not significantly increase the total energy consumption, but will likely result in a higher peak demand, affecting the sizes of both the power distribution system and energy storage, as well as utility demand charges.

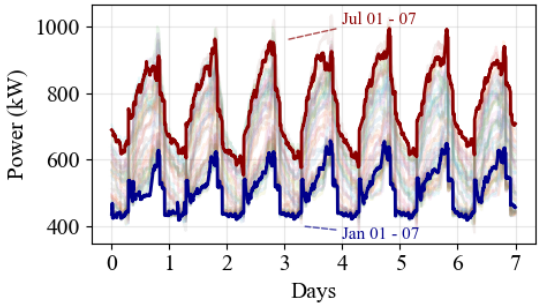

Figure 5. Building electrical load over a week for all weeks in a year.

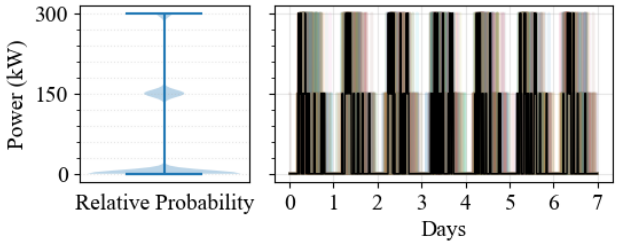

Figure 6. Violin plot (left) and weekly profile (right) of EV fast charging electrical load (one week shown as the dark line, remaining weeks in the background).

Utility Rate Structure

A utility rate tariff structure based on a high-price region (PG&E in Northern California) is used. The demand and energy prices are shown in Figure 7.

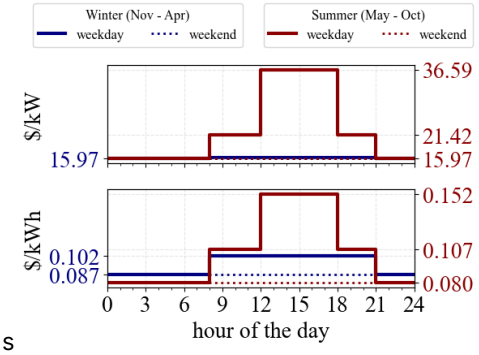

s

Figure 7. Utility rate tariff: demand (top) and energy (bottom) prices.

Location/Weather Inputs

The most relevant location-dependent weather parameters are presented in Figure 8, namely, ambient temperature (which drives the building energy consumption and equipment efficiency) and solar irradiance (which drives building heat gains and solar PV power generation). The city of Tucson, AZ, was chosen as the location for the study.

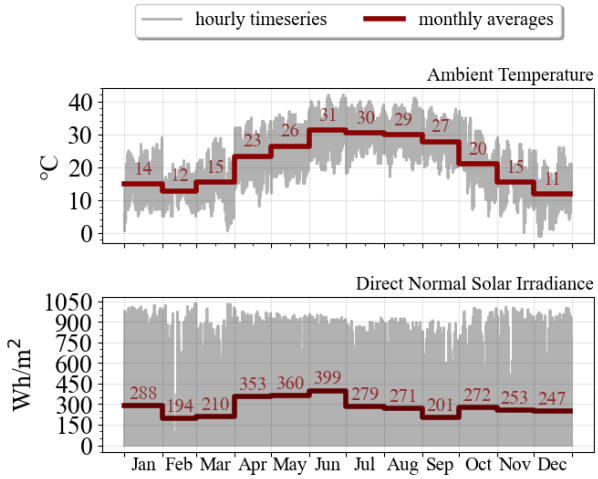

Figure 8. Weather inputs.

Remaining Inputs

A summary of the remaining inputs and settings is presented in Table 2.

Table 2: Remaining inputs.

Input	Value
Life-cycle Analysis Horizon	20 years
Discount Rate	8.3%
Battery Installed Cost	$540/kW + $120/kWh
PV Installed Cost	$1600/kW
PV initial range	0 – 2,000 kW
Battery initial range	0 – 5,000 kW 0 – 10,000 kWh
Forecast Method	Perfect
PV annual degradation	0.5%
Battery usable SOC range	10 – 90%
Battery Chemistry	LMO-LTO
Battery cost de-escalation rate for replacement	6%/year
Battery replacement capacity threshold	60%
MPC time horizon	24 h
MPC time step	1 min
MPC demand charge time averaging	15 min

RESULTS

The problem was solved using NREL's high-performance computing system Kestrel with dual socket Intel Xeon Sapphire Rapids (52-core) processors, 104 cores per CPU node, and 256 GB DDR5 memory. The sequential grid method was applied with 5 points and 6 iterations, achieving an accuracy upper bound of 0.8% of the initial range (or lower).

Design Solution: System Sizes and Costs

The main results of the analysis are presented in Table 3 for the base case (without BTMR), and the BTMR case (both cases with the EV charging station). The identified BTRM system consists of a battery with 390.6 kW capacity and 8.7 hours of duration, and a PV capacity of 1625 kW, highlighting the potential for PV deployment in locations with high solar incidence. Their associated capital costs follow a similar trend, being dominated by the large PV deployment and its higher unit cost. In this setting, the EV supply equipment (EVSE) capital cost is only a fraction of the BTMR system (which is not always the case, specially for commercial fleets). The benefits of BTMR deployment are shown in the metrics associated with electricity consumption and utility costs. Annual energy and peak demand are significantly reduced (by over half), in turn reducing their associated utility-related charges. The Levelized Cost of Charging (LCOC) (as defined in [13]) demonstrates the positive impact that BTMR systems can have on fast charging station deployment, decreasing from $0.33/kWh (a typical value in the US) to -$0.96/kWh (negative value representing the fact that the BTMR system reduces the total operating cost more than the EVSE increases it). Finally, the lifecycle net-present cost (adjusted capital and operating cost) indicates that the BTMR system increases profit gains by $1.41 million over the system's lifetime.

Sensitivity Analysis

One of the benefits of evaluating a grid of points (as opposed to a narrow search employed by most derivative-based methods) is that the sensitivity of the objective with respect to the decision variables can be evaluated. This allows the decision maker to identify design solutions with low sensitivity (in which adjusting a design variable does not significantly affect the objective function), adding more flexibility and confidence to the final design solution. Figure 9 shows contour plots of net-present cost with respect to two decision variables at a time (fixing the remaining one at its optimal value). Black dots represent points evaluated during the design procedure, while contour lines are generated performing interpolation using cubic radial-basis functions (RBF). The top-left plot shows a balanced effect between the two variables, with nonconvexities arising for large battery duration values. The top-right plot indicates that the battery power affects the design solution more significantly than PV size (contour lines are closer to each other). A similar trend is observed in the bottom-left plot, where battery power seems to affect the objective more significantly than battery capacity/duration. The ripples and non-convexities shown in the contour lines (more pronounced in the top-left plot) indicate a possibly low quality of the interpolation fit. One way of improving it would be to use a larger number of grid points in the design method.

Table 3: Overview of results: system sizes and costs.

Variable	Base Case	BTMR
System Sizes		
Battery Power	--	390.6 kW
Battery Storage (Duration)	--	3398.44 kWh (8.7 h)
PV Power	--	1625.0 kW
Capital Costs		
Battery Capital Cost	--	$618,750
PV Capital Cost	--	$2,600,000
EVSE Capital Cost	$308,400	$308,400
Electricity Consumption		
Energy from Grid	5,392 MWh/year	2,280 MWh/year
Monthly Peak Demand	1031.81 kW max 891.65 kW mean	695.39 kW max 579.62 kW mean
Utility Costs		
Energy charges	$527,449/year	$193,558/year
Demand charges	$321,538/year	$147,930/year
Levelized Costs		
EV Charging	$0.33/kWh	-$0.96/kWh
Energy (Electricity)	$0.16/kWh	$0.13/kWh
Lifecycle Costs		
Net Present Cost	$8.33 M	$6.92 M
Net Present Value	--	$1.41 M

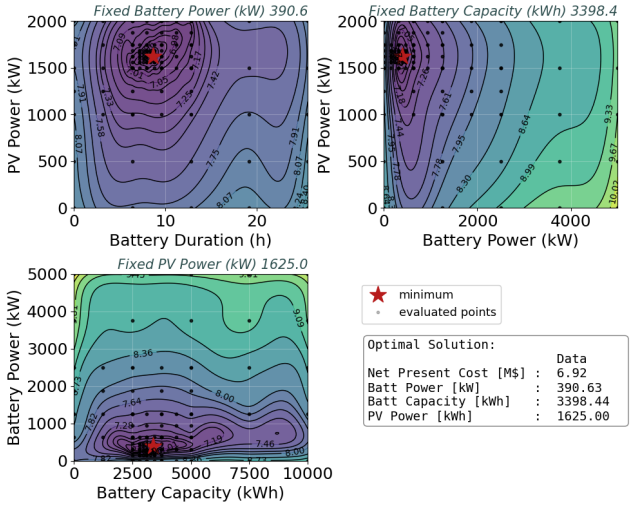

Figure 9. Contour plots of net present cost with respect to system design variables.

Dispatch and Load Profiles

The storage dispatch and load profiles (PV generation, building and EV loads, and power purchased from or sold to the grid) are presented in Figure 10. The first two subplots highlight the synergistic effect between battery

storage and PV generation, the former being discharged soon after the latter starts to decrease. The timing between PV generation and the building and EV charging loads also works in favor of BTMR, allowing most of the solar electricity generated onsite to be directly used to address the load. Finally, the power purchased from the grid shows a significant reduction in peak power demand (as well as energy consumption), inverting the time in which it happens from day to night, and the utilization of the net-metering mechanism to sell electricity back to the grid (despite its price being substantially lower than the purchase) during periods with solar generation surplus.

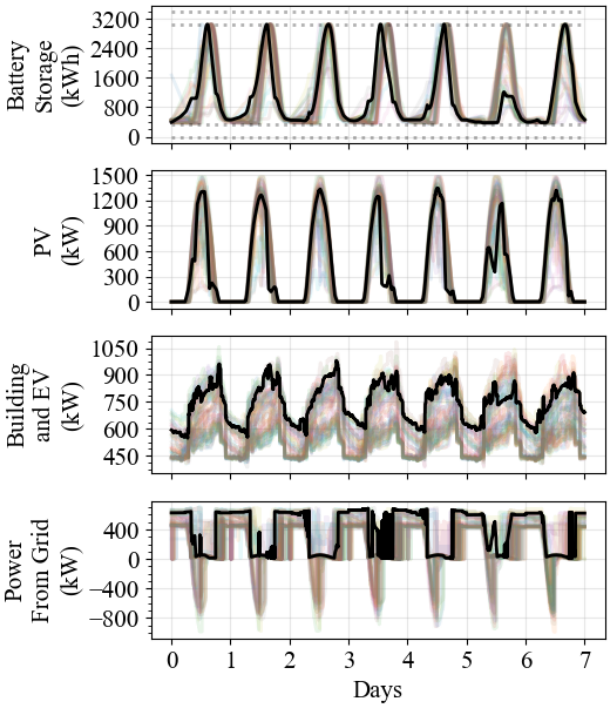

Figure 10. Dispatch and load profiles over all weeks in a year (week 26 highlighted as the dark solid line).

Resiliency against power outages

The cost-optimal BTMR system sized in the previous section also has the added benefit of providing resiliency against grid interruptions. That is, whenever there is an interruption in the power grid service (average of 4 hours, 1.4 times per year in the United States [16]), the battery storage (and PV generation) can be used to meet the system's electrical load. However, since the battery operates according to a cost-optimal dispatch, there is no guarantee that it will be able to meet that load. To assess this, the battery's SOC at all time steps in the simulated year was used to estimate its resiliency potential (how many time steps into the future it would be able to meet the system's load). The result is a probability distribution of resiliency hours, presented in Figure 11. The bar plots show the resiliency histogram with two levels of time step granularity (hourly and 15-min intervals). This graph represents the probability that the provided resiliency will be inside of each time interval (e.g., 29% between 0 and 1 hours, or 21% between 45 and 60 minutes). The solid line represents the inverse cumulative distribution function (with 15-min intervals), or the probability that the BTMR will provide over n hours of resiliency (e.g., 75% of the time the system provides over 1 hour of resiliency). The BTMR system provides over 30 minutes of resiliency 100% of the time, meaning that it can naturally address small outages without having to change its dispatching priorities, and can potentially meet up to 23 hours of future load.

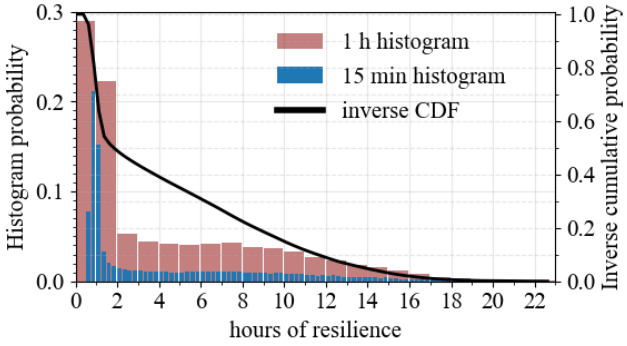

Figure 11. Resiliency provided by the cost-optimally-sized BTMR (battery + PV).

CONCLUSIONS

In this work, the optimal integrated design and dispatch of Behind-the-Meter Resources (BTMR) (i.e., battery energy store and PV generation) for retail commercial buildings with EV fast charging stations was addressed. A novel modeling framework was proposed, integrating detailed simulation models (of building, electric vehicle fast charging station, and BTMR equipment), model predictive control (MPC) strategies for equipment dispatch with closed-loop implementation, and a derivative-free design layer that leverages parallelization and high-performance computing. A sequential grid search method was employed to solve the design problem, balancing accuracy and computational effort. Results from a case study involving a big-box grocery store retail building model highlight the benefits of BTMR in reducing energy and peak demand charges, by generating clean electricity onsite, and shifting power purchases from the electric grid. Contour plots of lifecycle cost, generated by leveraging the parallel evaluations from the design method, indicate the design variables that have the biggest impact on the objective. Finally, the system's resiliency under grid outages was also evaluated, demonstrating a good potential for replacing fuel-based alternatives.

Ideas for future work include expanding the case

study to assess the potential of BTMR for retail buildings across multiple locations and utility rates; including a resiliency-based cost in the dispatch objective; considering the effect of forecast errors of future electrical load (from both building and EV charging station) in the control problem; and including carbon emissions in the design and dispatch optimization objectives.

ACKNOWLEDGEMENTS

Funding provided by the U.S. Department of Energy Vehicle Technologies Office, Buildings Technologies Office, the Assistant Secretary for Energy Efficiency and Renewable Energy.

REFERENCES

1. U.S. Environmental Protection Agency (EPA). Fast Facts on Transportation Greenhouse Gas Emissions. (2023) https://www.epa.gov/greenvehicles/fast-facts-transportation-greenhouse-gas-emissions
2. Gilleran M, Bonnema E, Woods J, Mishra P, Doebber I, Hunter C, Mitchell M, Mann M. Impact of electric vehicle charging on the power demand of retail buildings. *Adv. Appl. Energy* 4:100062 (2021).
3. NREL. Behind-the-Meter Storage Consortium. (N.D.) https://www.nrel.gov/research/behind-the-meter-storage-consortium.html
4. Ogunmodede O, Anderson K, Cutler D, Newman A. Optimizing design and dispatch of a renewable energy system. *Appl. Energy* 287:116527 (2021)
5. Mashayekh, S, Michael S, Gonçalo C, Heleno M. A mixed integer linear programming approach for optimal DER portfolio, sizing, and placement in multi-energy microgrids. *Appl. Energy*, 187:154-168 (2017)
6. EPRI. Distributed Energy Resource Value Estimation Tool (DER-VET™ v1.2), Program 94. https://www.der-vet.com/
7. NREL. EVI-EDGES: Electric Vehicle Infrastructure – Enabling Distributed Generation Energy Storage Model. (N.D.) https://www.nrel.gov/transportation/evi-edges.html
8. Guittet D, Bonnema E, Mitchell M, Mahvi A, Woods J. To freeze or not to freeze: model-predictive vs. schedule-based control of an ice-based thermal energy storage system. *Submitted*.
9. NREL. EVI-EnSite: Electric Vehicle Infrastructure – Energy Estimation and Site Optimization Tool. (N.D.) https://www.nrel.gov/transportation/evi-ensite.html
10. NREL. System Advisor Model Version 2022.11.29 (SAM 2022.11.21). https://https://sam.nrel.gov
11. NREL. System Advisor Model - Photovoltaic Models. (N.D.) https://sam.nrel.gov/photovoltaic.html
12. NREL. PVWatts Calculator. (N.D.) https://pvwatts.nrel.gov/
13. Guittet DL, Gasper P, Shirk M, Mitchell M, Gilleran M, Bonnema E, Smith K, Mishra P, Mann M. Levelized cost of charging of extreme fast charging with stationary LMO/LTO batteries. *J. Energy Storage* 82:110568 (2024)
14. Conn AR, Scheinberg K, Vicente LN. Introduction to Derivative-Free Optimization. Philadelphia: SIAM. (2009)
15. Larson J, Menickelly M, Wild SM. Derivative-Free Optimization Methods. Cambridge University Press. (2019)
16. U.S. Energy Information Administration (EIA). Reliability Metrics of U.S. Distribution System. (2023) https://www.eia.gov/electricity/annual/html/epa_11_01.html